THERMODYNAMICS OF PHOSPHORUS GRAIN BOUNDARY SEGREGATION IN LOW ALLOY STEELS

JOZEF JANOVEC[1]*, VRATKO VOKÁL[2], JANA KRESŤANKOVÁ[3],
PETER ŠEVC[2], ANNA VÝROSTKOVÁ[2]

Experimentally determined values of grain boundary and bulk concentrations of P, Cr, V, Mo, and Fe for Cr, Cr-V, and Cr-V-Mo steels aged at 773 and 823 K for 5000 h were used to calculate thermodynamic parameters ($\Delta H_{\mathrm{P}}^{0}$, $\Delta S_{\mathrm{P}}^{0}$, α'_{PCr}, α'_{PMo}, and α'_{PV}) of phosphorus segregation. The enrichment of segregating species at grain boundaries were measured on freshly fractured surfaces by means of Auger electron spectroscopy. Altogether 30 equations reflecting the site competition effect, Fowler-type binary interaction, and P-Cr, P-V, and P-Mo ternary interactions in all possible combinations were proposed for systems corresponding to the investigated steels. With respect to the recently published results, experimental data were fitted by 15 equations free of Fowler term. There was confirmed a linear relationship between enthalpy and entropy of phosphorus segregation. The consideration of P-Mo interaction in the calculations led to the less negative values of segregation enthalpy. There was recorded a high scatter of α'_{PCr}, α'_{PV}, and α'_{PMo} values calculated according to the different segregation equations. It was shown that the higher a number of ternary interactions considered the higher a scatter of values of interaction coefficients.

Key words: phosphorus grain boundary segregation, low alloy steels, Auger electron spectroscopy, segregation equations, thermodynamic parameters

TERMODYNAMIKA SEGREGÁCIE FOSFORU NA HRANICIACH ZŔN V NÍZKOLEGOVANÝCH OCELIACH

Experimentálne stanovené hodnoty koncentrácie P, Cr, V, Mo a Fe na hraniciach zŕn a v objeme pre Cr, Cr-V a Cr-V-Mo ocele žíhané pri 773 a 823 K v trvaní 5000 h

---

[1] Department of Materials Engineering, Slovak University of Technology, Bottova 24, 917 24 Trnava, Slovak Republic

[2] Institute of Materials Research, Slovak Academy of Sciences, Watsonova 47, 043 53 Košice, Slovak Republic

[3] Department of Experimental Physics, University of P. J. Šafárik, Park Angelinum 9, 041 54 Košice, Slovak Republic

* corresponding author, e-mail: `janovec@mtf.stuba.sk`

sme použili na výpočet termodynamických parametrov (ΔH^0_P, ΔS^0_P, α'_PCr, α'_PMo a α'_PV) charakterizujúcich segregáciu fosforu. Obohatenie hraníc zŕn segregujúcimi prvkami sme merali na čerstvo porušených povrchoch pomocou Augerovej elektrónovej spektroskopie. Pre systémy zodpovedajúce skúmaným oceliam sme navrhli celkom 30 rovníc, zohľadňujúcich konkurenčný efekt, binárnu interakciu fowlerovského typu a ternárne interakcie typu P-Cr, P-V a P-Mo vo všetkých možných kombináciách. S ohľadom na nedávno publikované výsledky experimentálne hodnoty sme fitovali 15 rovnicami, ktoré neobsahovali Fowlerov člen. Potvrdila sa lineárna závislosť medzi entalpiou a entropiou segregácie fosforu. Zohľadnenie interakcie P-Mo vo výpočtoch viedlo k menej negatívnym hodnotám segregačnej entalpie. Zaznamenali sme veľký rozptyl v hodnotách α'_PCr, α'_PV a α'_PMo vypočítaných podľa rôznych segregačných rovníc. Ukázalo sa, že čím väčší je počet uvažovaných ternárnych interakcií, tým väčší je aj rozptyl v hodnotách interakčných koeficientov.

1. Introduction

In the first half of 20th century grain boundaries were found to be an important factor influencing the behaviour of polycrystalline materials [1]. Since that time the intensive studies of structure (including electronic structure) and chemical composition of grain boundaries have been done.

1.1 Models of grain boundary structure

From the historical point of view, models of grain boundaries can be divided into three groups: dislocation-base models, models of transition area, and atomic models.

Models of the first group reflect the fundamental work of Read and Shockley [2] concerning the dislocation theory. In the basic theoretical consideration of a tilt small-angle boundary [3] the joining of two crystals with ideal surfaces was supposed. If they are brought together, atoms in the newly formed boundary will accommodate to both lattices in a manner best described as a dislocation array. Physical reason for the formation of small-angle boundaries is the cancellation of long-range strain fields of individual dislocations in the term of strain-field interaction [4]. Two grains separated by a twist small-angle boundary are rotated relative to one another about the axis perpendicular to the plane of boundary. The twist small-angle boundaries are formed by 2 or 3 sets of screw dislocations [3, 5]. The dislocation model of a high-angle boundary [6] is very similar to that of the tilt small-angle boundary. If dislocations are uniformly spaced in the boundary plane, a low-energy interface is assumed to be formed. The high-angle boundary with uniform dislocation spacing can only exist when the dislocation spacing is equal to an integer number of lattice planes terminating the boundary. Unfortunately, boundary dislocations in real materials show different properties as suggested in the model. A "non-ideal behaviour" of the boundary dislocations consisting in their "overlapping" and interaction is mainly caused by higher dislocation density near the boundaries.

The first transition area model of grain boundary was proposed by Rosenhain and Ewen [7] about hundred years ago. A grain boundary in the model was suggested to be an amorphous cement foil of thickness about 100 atomic layers. Later, the transition lattice [8], coincidence lattice [9], polyhedral unit [10], and structural unit [11] models were proposed. The last of them seems to be the most credible. It is based on the suggestion that two crystals forming a coincidence boundary relax by shear-type displacement (rigid-body relaxation) leading to the formation of even atom configurations (so-called structural units) along the boundary.

In atomic models, the energy balance between atoms of the grain boundary is considered. The structure-energy correlation for free surfaces was described by Herring [12] using so-called broken-bond concept. The same approach was applied by Wolf and Yip [13] for the characterisation of grain boundaries in polycrystalline materials.

1.2 Chemistry of grain boundaries

Diffusion-related phenomena like segregation are mostly responsible for chemical changes at grain boundaries. A fundamental relationship between the surface tension (free energy) and chemical state of an adsorbate (segregated) surface was proposed by Gibbs [14]. Gibbs considered in his concept so-called "dividing surface" enabling discontinuous transition between adjacent surface layers. This is not acceptable for internal surfaces, because the physico-chemical properties of the solid state vary continuously from one homogeneous phase to the adjoining phase. Guggenheim [15] therefore suggested to consider the internal surface as a separate homogeneous phase of finite thickness. A significant progress in the development of thermodynamics of equilibrium segregation is associated with McLean [16]. The originally non-interactive McLean theory was later modified by Guttmann [17] who introduced so-called binary (between atoms of the same element) and ternary (between atoms of different solute elements) interactions. Guttmann and McLean [18] proposed altogether five models of equilibrium segregation for multicomponent systems. In these models, they considered not only different types of interactions, but also the site competition effect, formation of quasimolecules (stable clusters consisting of two atoms), and precipitation of two-dimensional compounds in grain boundaries.

1.3 Aims of the article

It is generally known that the small structural or compositional changes at grain boundaries can strongly affect mechanical, chemical and physical properties of polycrystalline materials. This is, because grain boundaries form three-dimensional net spread through the whole volume of a body. If their structure and chemical composition is inconvenient, the properties of polycrystals are changed and become more sensitive to the intergranular fracture. A positive correlation between the portion of intergranular fracture or shift in the transition temperature to more positive values on the one side and the grain boundary concentration of some impurities (e. g. phosphorus) on the other side was evidenced by many authors [1, 19, 20]. To control the process of intergranular fracture in polycrystalline materials, the quantification of impurity segregation is important. The possible way how to make it is the application of segregation theories to polycrystals and the determination of corresponding thermodynamic parameters (e. g. segregation enthalpy and entropy, interaction coefficients).

Reflecting the above ideas, the main aim of the present article is to specify the ability of different segregation theories and equations for the quantification of phosphorus segregation in different types of low alloy steels.

2. Experimental

Ingots of three low alloy steels differing in chromium, molybdenum, and vanadium contents (Table 1) were hot forged between 1373 and 1123 K into bars with cross section of 12 × 12 mm. Subsequently, samples of 12 × 12 × 50 mm were austenitised at 1523 K for 0.75 h to achieve polycrystals with the average size of prior austenite grains about 0.3 mm [21]. After austenitising the samples were quenched into a water solution of KOH, tempered at 923 K for 2 h, water cooled, aged at 773 and 823 K for 5000 h, and repeatedly water cooled. Before tempering and ageing they were placed into evacuated silica capsules.

Table 1. Chemical composition of investigated Cr, Cr-V, and Cr-Mo-V steels. Mass contents of elements are given in %

Steel	C	Mn	Si	Cr	Mo	V	P	S	N	Fe
Cr	0.115	0.333	0.234	0.894	–	–	0.045	0.004	0.004	bal.
Cr-V	0.134	0.332	0.228	0.881	–	0.507	0.040	0.004	0.002	bal.
Cr-Mo-V	0.126	0.321	0.223	0.851	0.405	0.254	0.045	0.223	0.003	bal.

From the aged samples notched cylindrical specimens (ø 3 × 15 mm) were machined. The specimens were fractured in situ by impact at 163 K in an ultrahigh-vacuum chamber ($\leq 10^{-7}$ Pa) of a scanning Auger microprobe. Intergranular facets achieved (Fig. 1a) were analysed immediately using the primary electron beam of following parameters: voltage of 5 kV, electron beam current of 60 nA, and beam diameter about 0.5 μm.

In Auger spectra of Cr-Mo-V steel, peaks of phosphorus, molybdenum, carbon, vanadium, chromium, oxygen, and iron were collected (Fig. 1b). In the spectra corresponding to Cr-V and Cr steels, peaks of molybdenum and molybde-

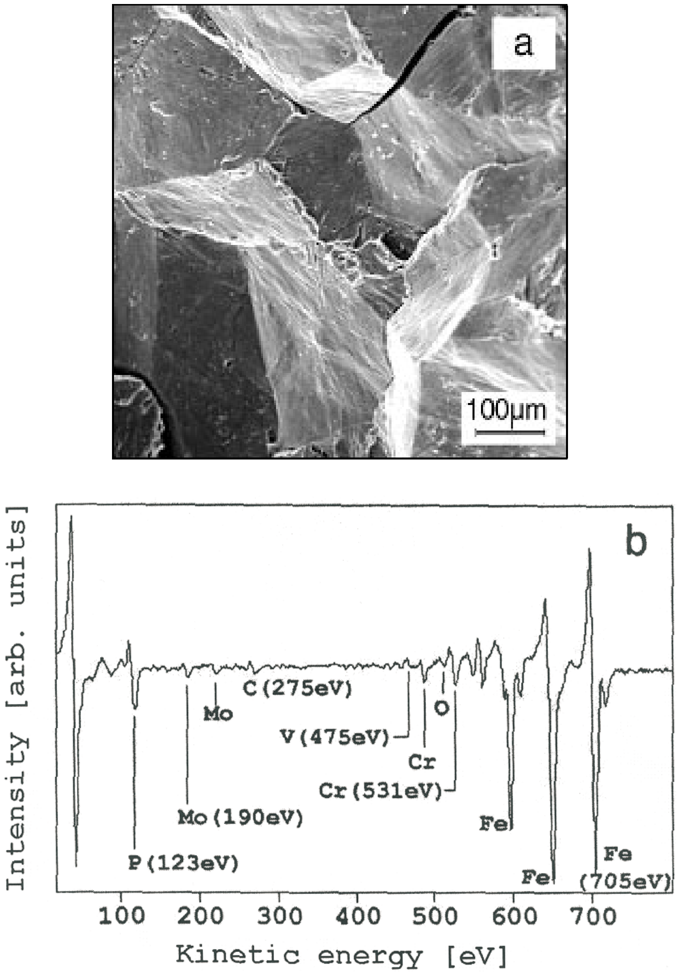

Fig. 1. Intergranular facets characteristic for low-temperature fracture (at 163 K) of Cr-Mo-V steel after ageing at 723 or 823 K for 5000 h: a) SEM micrograph, b) corresponding Auger spectrum.

num + vanadium are missing, respectively. Peak heights of $\mathrm{P}_{123\mathrm{eV}}$ (K_{P}), $\mathrm{Mo}_{190\mathrm{eV}}$ (K_{Mo}), $\mathrm{V}_{475\mathrm{eV}}$ (K_{V}), $\mathrm{Cr}_{531\mathrm{eV}}$ (K_{Cr}), and $\mathrm{Fe}_{705\mathrm{eV}}$ (K_{Fe}), were used to calculate the grain boundary concentrations of phosphorus ($X_{\mathrm{P}}^{\mathrm{S}}$), chromium ($X_{\mathrm{Cr}}^{\mathrm{S}}$), molybdenum ($X_{\mathrm{Mo}}^{\mathrm{S}}$), and vanadium ($X_{\mathrm{V}}^{\mathrm{S}}$) according to the standard equation [22]:

$$X_i^{\mathrm{S}} = \frac{K_i}{S_i}\left(\sum_j \frac{K_j}{S_j}\right)^{-1}, \tag{1}$$

where S_i, S_j are the relative Auger sensitivities of the corresponding elements i, j = P, Mo, Cr, V, and Fe. Because of the contamination from the residual gas atmosphere and the occurrence of carbide particles at grain boundaries, the carbon and oxygen peaks were not taken into account in the calculations.

Scanning electron microscopy (SEM) was used to document morphology of the investigated fracture surfaces.

3. Theoretical outlines

From historical point of view, the first integral segregation theory applicable for internal surfaces (grain boundaries) in binary dilute m-i system was proposed by McLean [16]:

$$\frac{X_i^{\mathrm{S}}}{1 - X_i^{\mathrm{S}}} = \frac{X_i^{\mathrm{B}}}{1 - X_i^{\mathrm{B}}} \mathrm{e}^{-\frac{G_i^0}{RT}}. \tag{2}$$

In the above Langmuir-McLean equation (2), terms X_i^{S} and X_i^{B} represent the equilibrium grain boundary and bulk concentrations of the solute i, respectively. Term R represents the gas constant. Gibbs free energy of i-segregation in binary m-i system at temperature T is expressed by the term ΔG_i^0. According to the rules of fundamental thermodynamics, it can also be written:

$$\Delta G_i^0 = \Delta H_i^0 - T \Delta S_i^0, \tag{3}$$

where ΔH_i^0 and ΔS_i^0 are enthalpy and entropy of i-segregation in binary m-i system.

Guttmann [17, 18] proposed the most general segregation theory represented by couple of equations:

$$\frac{X_i^{\mathrm{S}}}{1 - X_i^{\mathrm{S}} - \sum\limits_{j \neq i,m} X_j^{\mathrm{S}}} = \frac{X_i^{\mathrm{B}}}{1 - X_i^{\mathrm{B}} - \sum\limits_{j \neq i,m} X_j^{\mathrm{B}}} \mathrm{e}^{-\frac{G_i}{RT}}, \tag{4}$$

$$\Delta G_i = \Delta H_i^0 - T \Delta S_i^0 - 2\alpha_{im}(X_i^{\mathrm{S}} - X_i^{\mathrm{B}}) + \sum_{j \neq i,m} \alpha'_{ij}(X_j^{\mathrm{S}} - X_j^{\mathrm{B}}). \tag{5}$$

The theory should be applicable for the characterisation of equilibrium grain boundary segregation of a solute i in a multicomponent m-base system. Both the non-interactive site competition effect (see denominators in concentration terms of Eq. 4) and the chemical interactions (see last two terms of Eq. 5) are considered in the theory. Fowler type binary i-i interaction and ternary i-j interaction (j represents the third element in m-base system containing solute i) are included in the energy term, ΔG_i, representing the Gibbs free energy of segregation for a

Table 2. Possible equations characterizing the phosphorus segregation in Fe-base systems containing Cr, V, and/or Mo. For descriptions of possibilities see chapter 3. First part: I – XII

<table>
<tr><td><i>Equation:</i> I</td><td><i>Possibilities:</i> 1a, 2b, 3b, 4b</td><td><i>Steels:</i> Cr, Cr-V, Cr-V-Mo</td></tr>
<tr><td colspan="3">$$-RT\ln\frac{(1-X_{\mathrm{P}}^{\mathrm{B}})\,X_{\mathrm{P}}^{\mathrm{S}}}{X_{\mathrm{P}}^{\mathrm{B}}(1-X_{\mathrm{P}}^{\mathrm{S}})}=\Delta H_{\mathrm{P}}^{0}-\Delta S_{\mathrm{P}}^{0}T$$</td></tr>
<tr><td><i>Equation:</i> II</td><td><i>Possibilities:</i> 1a, 2b, 3a, 4b</td><td><i>Steels:</i> Cr, Cr-V, Cr-V-Mo</td></tr>
<tr><td colspan="3">$$-RT\ln\frac{(1-X_{\mathrm{P}}^{\mathrm{B}})\,X_{\mathrm{P}}^{\mathrm{S}}}{X_{\mathrm{P}}^{\mathrm{B}}(1-X_{\mathrm{P}}^{\mathrm{S}})}=\Delta H_{\mathrm{P}}^{0}-\Delta S_{\mathrm{P}}^{0}T-2\alpha_{\mathrm{PFe}}(X_{\mathrm{P}}^{\mathrm{S}}-X_{\mathrm{P}}^{\mathrm{B}})$$</td></tr>
<tr><td><i>Equation:</i> III</td><td><i>Possibilities:</i> 1b, 2b, 3b, 4a</td><td><i>Steels:</i> Cr, Cr-V, Cr-V-Mo</td></tr>
<tr><td colspan="3">$$-RT\ln\frac{(1-X_{\mathrm{P}}^{\mathrm{B}})\,X_{\mathrm{P}}^{\mathrm{S}}}{X_{\mathrm{P}}^{\mathrm{B}}(1-X_{\mathrm{P}}^{\mathrm{S}})}=\Delta H_{\mathrm{P}}^{0}-\Delta S_{\mathrm{P}}^{0}T+\alpha'_{\mathrm{PCr}}(X_{\mathrm{Cr}}^{\mathrm{S}}-X_{\mathrm{Cr}}^{\mathrm{B}})$$</td></tr>
<tr><td><i>Equation:</i> IV</td><td><i>Possibilities:</i> 1b, 2b, 3a, 4a</td><td><i>Steels:</i> Cr, Cr-V, Cr-V-Mo</td></tr>
<tr><td colspan="3">$$-RT\ln\frac{(1-X_{\mathrm{P}}^{\mathrm{B}})\,X_{\mathrm{P}}^{\mathrm{S}}}{X_{\mathrm{P}}^{\mathrm{B}}(1-X_{\mathrm{P}}^{\mathrm{S}})}=\Delta H_{\mathrm{P}}^{0}-\Delta S_{\mathrm{P}}^{0}T-2\alpha_{\mathrm{PFe}}(X_{\mathrm{P}}^{\mathrm{S}}-X_{\mathrm{P}}^{\mathrm{B}})+\alpha'_{\mathrm{PCr}}(X_{\mathrm{Cr}}^{\mathrm{S}}-X_{\mathrm{Cr}}^{\mathrm{B}})$$</td></tr>
<tr><td><i>Equation:</i> V</td><td><i>Possibilities:</i> 1b, 2a, 3b, 4a</td><td><i>Steels:</i> Cr, Cr-V, Cr-V-Mo</td></tr>
<tr><td colspan="3">$$-RT\ln\frac{(1-X_{\mathrm{P}}^{\mathrm{B}}-X_{\mathrm{Cr}}^{\mathrm{B}})\,X_{\mathrm{P}}^{\mathrm{S}}}{X_{\mathrm{P}}^{\mathrm{B}}(1-X_{\mathrm{P}}^{\mathrm{S}}-X_{\mathrm{Cr}}^{\mathrm{S}})}=\Delta H_{\mathrm{P}}^{0}-\Delta S_{\mathrm{P}}^{0}T+\alpha'_{\mathrm{PCr}}(X_{\mathrm{Cr}}^{\mathrm{S}}-X_{\mathrm{Cr}}^{\mathrm{B}})$$</td></tr>
<tr><td><i>Equation:</i> VI</td><td><i>Possibilities:</i> 1b, 2a, 3a, 4a</td><td><i>Steels:</i> Cr, Cr-V, Cr-V-Mo</td></tr>
<tr><td colspan="3">$$-RT\ln\frac{(1-X_{\mathrm{P}}^{\mathrm{B}}-X_{\mathrm{Cr}}^{\mathrm{B}})\,X_{\mathrm{P}}^{\mathrm{S}}}{X_{\mathrm{P}}^{\mathrm{B}}(1-X_{\mathrm{P}}^{\mathrm{S}}-X_{\mathrm{Cr}}^{\mathrm{S}})}=\Delta H_{\mathrm{P}}^{0}-\Delta S_{\mathrm{P}}^{0}T-2\alpha_{\mathrm{PFe}}(X_{\mathrm{P}}^{\mathrm{S}}-X_{\mathrm{P}}^{\mathrm{B}})+\alpha'_{\mathrm{PCr}}(X_{\mathrm{Cr}}^{\mathrm{S}}-X_{\mathrm{Cr}}^{\mathrm{B}})$$</td></tr>
<tr><td><i>Equation:</i> VII</td><td><i>Possibilities:</i> 1c, 2b, 3b, 4a</td><td><i>Steels:</i> Cr-V, Cr-V-Mo</td></tr>
<tr><td colspan="3">$$-RT\ln\frac{(1-X_{\mathrm{P}}^{\mathrm{B}})\,X_{\mathrm{P}}^{\mathrm{S}}}{X_{\mathrm{P}}^{\mathrm{B}}(1-X_{\mathrm{P}}^{\mathrm{S}})}=\Delta H_{\mathrm{P}}^{0}-\Delta S_{\mathrm{P}}^{0}T+\alpha'_{\mathrm{PV}}(X_{\mathrm{V}}^{\mathrm{S}}-X_{\mathrm{V}}^{\mathrm{B}})$$</td></tr>
<tr><td><i>Equation:</i> VIII</td><td><i>Possibilities:</i> 1c, 2b, 3a, 4a</td><td><i>Steels:</i> Cr-V, Cr-V-Mo</td></tr>
<tr><td colspan="3">$$-RT\ln\frac{(1-X_{\mathrm{P}}^{\mathrm{B}})\,X_{\mathrm{P}}^{\mathrm{S}}}{X_{\mathrm{P}}^{\mathrm{B}}(1-X_{\mathrm{P}}^{\mathrm{S}})}=\Delta H_{\mathrm{P}}^{0}-\Delta S_{\mathrm{P}}^{0}T-2\alpha_{\mathrm{PFe}}(X_{\mathrm{P}}^{\mathrm{S}}-X_{\mathrm{P}}^{\mathrm{B}})+\alpha'_{\mathrm{PV}}(X_{\mathrm{V}}^{\mathrm{S}}-X_{\mathrm{V}}^{\mathrm{B}})$$</td></tr>
<tr><td><i>Equation:</i> IX</td><td><i>Possibilities:</i> 1c, 2a, 3b, 4a</td><td><i>Steels:</i> Cr-V, Cr-V-Mo</td></tr>
<tr><td colspan="3">$$-RT\ln\frac{(1-X_{\mathrm{P}}^{\mathrm{B}}-X_{\mathrm{V}}^{\mathrm{B}})\,X_{\mathrm{P}}^{\mathrm{S}}}{X_{\mathrm{P}}^{\mathrm{B}}(1-X_{\mathrm{P}}^{\mathrm{S}}-X_{\mathrm{V}}^{\mathrm{S}})}=\Delta H_{\mathrm{P}}^{0}-\Delta S_{\mathrm{P}}^{0}T+\alpha'_{\mathrm{PV}}(X_{\mathrm{V}}^{\mathrm{S}}-X_{\mathrm{V}}^{\mathrm{B}})$$</td></tr>
<tr><td><i>Equation:</i> X</td><td><i>Possibilities:</i> 1c, 2a, 3a, 4a</td><td><i>Steels:</i> Cr-V, Cr-V-Mo</td></tr>
<tr><td colspan="3">$$-RT\ln\frac{(1-X_{\mathrm{P}}^{\mathrm{B}}-X_{\mathrm{V}}^{\mathrm{B}})\,X_{\mathrm{P}}^{\mathrm{S}}}{X_{\mathrm{P}}^{\mathrm{B}}(1-X_{\mathrm{P}}^{\mathrm{S}}-X_{\mathrm{V}}^{\mathrm{S}})}=\Delta H_{\mathrm{P}}^{0}-\Delta S_{\mathrm{P}}^{0}T-2\alpha_{\mathrm{PFe}}(X_{\mathrm{P}}^{\mathrm{S}}-X_{\mathrm{P}}^{\mathrm{B}})+\alpha'_{\mathrm{PV}}(X_{\mathrm{V}}^{\mathrm{S}}-X_{\mathrm{V}}^{\mathrm{B}})$$</td></tr>
<tr><td><i>Equation:</i> XI</td><td><i>Possibilities:</i> 1d, 2b, 3b, 4a</td><td><i>Steel:</i> Cr-V-Mo</td></tr>
<tr><td colspan="3">$$-RT\ln\frac{(1-X_{\mathrm{P}}^{\mathrm{B}})\,X_{\mathrm{P}}^{\mathrm{S}}}{X_{\mathrm{P}}^{\mathrm{B}}(1-X_{\mathrm{P}}^{\mathrm{S}})}=\Delta H_{\mathrm{P}}^{0}-\Delta S_{\mathrm{P}}^{0}T+\alpha'_{\mathrm{PMo}}(X_{\mathrm{Mo}}^{\mathrm{S}}-X_{\mathrm{Mo}}^{\mathrm{B}})$$</td></tr>
<tr><td><i>Equation:</i> XII</td><td><i>Possibilities:</i> 1d, 2b, 3a, 4a</td><td><i>Steel:</i> Cr-V-Mo</td></tr>
<tr><td colspan="3">$$-RT\ln\frac{(1-X_{\mathrm{P}}^{\mathrm{B}})\,X_{\mathrm{P}}^{\mathrm{S}}}{X_{\mathrm{P}}^{\mathrm{B}}(1-X_{\mathrm{P}}^{\mathrm{S}})}=\Delta H_{\mathrm{P}}^{0}-\Delta S_{\mathrm{P}}^{0}T-2\alpha_{\mathrm{PFe}}(X_{\mathrm{P}}^{\mathrm{S}}-X_{\mathrm{P}}^{\mathrm{B}})+\alpha'_{\mathrm{PMo}}(X_{\mathrm{Mo}}^{\mathrm{S}}-X_{\mathrm{Mo}}^{\mathrm{B}})$$</td></tr>
</table>

Table 3. Possible equations characterizing the phosphorus segregation in Fe-base systems containing Cr, V, and/or Mo. For descriptions of possibilities see chapter 3. Second part: XIII – XXII

<table>
<tr><td><i>Equation:</i> XIII</td><td><i>Possibilities:</i> 1d, 2a, 3b, 4a</td><td><i>Steel:</i> Cr-V-Mo</td></tr>
<tr><td colspan="3">$-RT\ln\frac{(1-X_{\mathrm{P}}^{\mathrm{B}}-X_{\mathrm{Mo}}^{\mathrm{B}})\,X_{\mathrm{P}}^{\mathrm{S}}}{X_{\mathrm{P}}^{\mathrm{B}}(1-X_{\mathrm{P}}^{\mathrm{S}}-X_{\mathrm{Mo}}^{\mathrm{S}})}=\Delta H_{\mathrm{P}}^{0}-\Delta S_{\mathrm{P}}^{0}T+\alpha'_{\mathrm{PMo}}(X_{\mathrm{Mo}}^{\mathrm{S}}-X_{\mathrm{Mo}}^{\mathrm{B}})$</td></tr>
<tr><td><i>Equation:</i> XIV</td><td><i>Possibilities:</i> 1d, 2a, 3a, 4a</td><td><i>Steel:</i> Cr-V-Mo</td></tr>
<tr><td colspan="3">$\begin{gathered}-RT\ln\frac{(1-X_{\mathrm{P}}^{\mathrm{B}}-X_{\mathrm{Mo}}^{\mathrm{B}})\,X_{\mathrm{P}}^{\mathrm{S}}}{X_{\mathrm{P}}^{\mathrm{B}}(1-X_{\mathrm{P}}^{\mathrm{S}}-X_{\mathrm{Mo}}^{\mathrm{S}})}= \\ =\Delta H_{\mathrm{P}}^{0}-\Delta S_{\mathrm{P}}^{0}T-2\alpha_{\mathrm{PFe}}(X_{\mathrm{P}}^{\mathrm{S}}-X_{\mathrm{P}}^{\mathrm{B}})+\alpha'_{\mathrm{PMo}}(X_{\mathrm{Mo}}^{\mathrm{S}}-X_{\mathrm{Mo}}^{\mathrm{B}})\end{gathered}$</td></tr>
<tr><td><i>Equation:</i> XV</td><td><i>Possibilities:</i> 1e, 2b, 3b, 4a</td><td><i>Steels:</i> Cr-V, Cr-V-Mo</td></tr>
<tr><td colspan="3">$-RT\ln\frac{(1-X_{\mathrm{P}}^{\mathrm{B}})\,X_{\mathrm{P}}^{\mathrm{S}}}{X_{\mathrm{P}}^{\mathrm{B}}(1-X_{\mathrm{P}}^{\mathrm{S}})}=\Delta H_{\mathrm{P}}^{0}-\Delta S_{\mathrm{P}}^{0}T+\alpha'_{\mathrm{PCr}}(X_{\mathrm{Cr}}^{\mathrm{S}}-X_{\mathrm{Cr}}^{\mathrm{B}})+\alpha'_{\mathrm{PV}}(X_{\mathrm{V}}^{\mathrm{S}}-X_{\mathrm{V}}^{\mathrm{B}})$</td></tr>
<tr><td><i>Equation:</i> XVI</td><td><i>Possibilities:</i> 1e, 2b, 3a, 4a</td><td><i>Steels:</i> Cr-V, Cr-V-Mo</td></tr>
<tr><td colspan="3">$\begin{gathered}-RT\ln\frac{(1-X_{\mathrm{P}}^{\mathrm{B}})\,X_{\mathrm{P}}^{\mathrm{S}}}{X_{\mathrm{P}}^{\mathrm{B}}(1-X_{\mathrm{P}}^{\mathrm{S}})}= \\ =\Delta H_{\mathrm{P}}^{0}-\Delta S_{\mathrm{P}}^{0}T-2\alpha_{\mathrm{PFe}}(X_{\mathrm{P}}^{\mathrm{S}}-X_{\mathrm{P}}^{\mathrm{B}})+\alpha'_{\mathrm{PCr}}(X_{\mathrm{Cr}}^{\mathrm{S}}-X_{\mathrm{Cr}}^{\mathrm{B}})+\alpha'_{\mathrm{PV}}(X_{\mathrm{V}}^{\mathrm{S}}-X_{\mathrm{V}}^{\mathrm{B}})\end{gathered}$</td></tr>
<tr><td><i>Equation:</i> XVII</td><td><i>Possibilities:</i> 1e, 2a, 3b, 4a</td><td><i>Steels:</i> Cr-V, Cr-V-Mo</td></tr>
<tr><td colspan="3">$\begin{gathered}-RT\ln\frac{(1-X_{\mathrm{P}}^{\mathrm{B}}-X_{\mathrm{Cr}}^{\mathrm{B}}-X_{\mathrm{V}}^{\mathrm{B}})\,X_{\mathrm{P}}^{\mathrm{S}}}{X_{\mathrm{P}}^{\mathrm{B}}(1-X_{\mathrm{P}}^{\mathrm{S}}-X_{\mathrm{Cr}}^{\mathrm{S}}-X_{\mathrm{V}}^{\mathrm{S}})}= \\ =\Delta H_{\mathrm{P}}^{0}-\Delta S_{\mathrm{P}}^{0}T+\alpha'_{\mathrm{PCr}}(X_{\mathrm{Cr}}^{\mathrm{S}}-X_{\mathrm{Cr}}^{\mathrm{B}})+\alpha'_{\mathrm{PV}}(X_{\mathrm{V}}^{\mathrm{S}}-X_{\mathrm{V}}^{\mathrm{B}})\end{gathered}$</td></tr>
<tr><td><i>Equation:</i> XVIII</td><td><i>Possibilities:</i> 1e, 2a, 3a, 4a</td><td><i>Steels:</i> Cr-V, Cr-V-Mo</td></tr>
<tr><td colspan="3">$\begin{gathered}-RT\ln\frac{(1-X_{\mathrm{P}}^{\mathrm{B}}-X_{\mathrm{Cr}}^{\mathrm{B}}-X_{\mathrm{V}}^{\mathrm{B}})\,X_{\mathrm{P}}^{\mathrm{S}}}{X_{\mathrm{P}}^{\mathrm{B}}(1-X_{\mathrm{P}}^{\mathrm{S}}-X_{\mathrm{Cr}}^{\mathrm{S}}-X_{\mathrm{V}}^{\mathrm{S}})}= \\ =\Delta H_{\mathrm{P}}^{0}-\Delta S_{\mathrm{P}}^{0}T-2\alpha_{\mathrm{PFe}}(X_{\mathrm{P}}^{\mathrm{S}}-X_{\mathrm{P}}^{\mathrm{B}})+\alpha'_{\mathrm{PCr}}(X_{\mathrm{Cr}}^{\mathrm{S}}-X_{\mathrm{Cr}}^{\mathrm{B}})+\alpha'_{\mathrm{PV}}(X_{\mathrm{V}}^{\mathrm{S}}-X_{\mathrm{V}}^{\mathrm{B}})\end{gathered}$</td></tr>
<tr><td><i>Equation:</i> XIX</td><td><i>Possibilities:</i> 1f, 2b, 3b, 4a</td><td><i>Steel:</i> Cr-V-Mo</td></tr>
<tr><td colspan="3">$-RT\ln\frac{(1-X_{\mathrm{P}}^{\mathrm{B}})\,X_{\mathrm{P}}^{\mathrm{S}}}{X_{\mathrm{P}}^{\mathrm{B}}(1-X_{\mathrm{P}}^{\mathrm{S}})}=\Delta H_{\mathrm{P}}^{0}-\Delta S_{\mathrm{P}}^{0}T+\alpha'_{\mathrm{PCr}}(X_{\mathrm{Cr}}^{\mathrm{S}}-X_{\mathrm{Cr}}^{\mathrm{B}})+\alpha'_{\mathrm{PMo}}(X_{\mathrm{Mo}}^{\mathrm{S}}-X_{\mathrm{Mo}}^{\mathrm{B}})$</td></tr>
<tr><td><i>Equation:</i> XX</td><td><i>Possibilities:</i> 1f, 2b, 3a, 4a</td><td><i>Steel:</i> Cr-V-Mo</td></tr>
<tr><td colspan="3">$\begin{gathered}-RT\ln\frac{(1-X_{\mathrm{P}}^{\mathrm{B}})\,X_{\mathrm{P}}^{\mathrm{S}}}{X_{\mathrm{P}}^{\mathrm{B}}(1-X_{\mathrm{P}}^{\mathrm{S}})}= \\ =\Delta H_{\mathrm{P}}^{0}-\Delta S_{\mathrm{P}}^{0}T-2\alpha_{\mathrm{PFe}}(X_{\mathrm{P}}^{\mathrm{S}}-X_{\mathrm{P}}^{\mathrm{B}})+\alpha'_{\mathrm{PCr}}(X_{\mathrm{Cr}}^{\mathrm{S}}-X_{\mathrm{Cr}}^{\mathrm{B}})+\alpha'_{\mathrm{PMo}}(X_{\mathrm{Mo}}^{\mathrm{S}}-X_{\mathrm{Mo}}^{\mathrm{B}})\end{gathered}$</td></tr>
<tr><td><i>Equation:</i> XXI</td><td><i>Possibilities:</i> 1f, 2a, 3b, 4a</td><td><i>Steel:</i> Cr-V-Mo</td></tr>
<tr><td colspan="3">$\begin{gathered}-RT\ln\frac{(1-X_{\mathrm{P}}^{\mathrm{B}}-X_{\mathrm{Cr}}^{\mathrm{B}}-X_{\mathrm{Mo}}^{\mathrm{B}})\,X_{\mathrm{P}}^{\mathrm{S}}}{X_{\mathrm{P}}^{\mathrm{B}}(1-X_{\mathrm{P}}^{\mathrm{S}}-X_{\mathrm{Cr}}^{\mathrm{S}}-X_{\mathrm{Mo}}^{\mathrm{S}})}= \\ =\Delta H_{\mathrm{P}}^{0}-\Delta S_{\mathrm{P}}^{0}T+\alpha'_{\mathrm{PCr}}(X_{\mathrm{Cr}}^{\mathrm{S}}-X_{\mathrm{Cr}}^{\mathrm{B}})+\alpha'_{\mathrm{PMo}}(X_{\mathrm{Mo}}^{\mathrm{S}}-X_{\mathrm{Mo}}^{\mathrm{B}})\end{gathered}$</td></tr>
<tr><td><i>Equation:</i> XXII</td><td><i>Possibilities:</i> 1f, 2a, 3a, 4a</td><td><i>Steel:</i> Cr-V-Mo</td></tr>
<tr><td colspan="3">$\begin{gathered}-RT\ln\frac{(1-X_{\mathrm{P}}^{\mathrm{B}}-X_{\mathrm{Cr}}^{\mathrm{B}}-X_{\mathrm{Mo}}^{\mathrm{B}})\,X_{\mathrm{P}}^{\mathrm{S}}}{X_{\mathrm{P}}^{\mathrm{B}}(1-X_{\mathrm{P}}^{\mathrm{S}}-X_{\mathrm{Cr}}^{\mathrm{S}}-X_{\mathrm{Mo}}^{\mathrm{S}})}= \\ =\Delta H_{\mathrm{P}}^{0}-\Delta S_{\mathrm{P}}^{0}T-2\alpha_{\mathrm{PFe}}(X_{\mathrm{P}}^{\mathrm{S}}-X_{\mathrm{P}}^{\mathrm{B}})+\alpha'_{\mathrm{PCr}}(X_{\mathrm{Cr}}^{\mathrm{S}}-X_{\mathrm{Cr}}^{\mathrm{B}})+\alpha'_{\mathrm{Mo}}(X_{\mathrm{Mo}}^{\mathrm{S}}-X_{\mathrm{Mo}}^{\mathrm{B}})\end{gathered}$</td></tr>
</table>

Table 4. Possible equations characterizing the phosphorus segregation in Fe-base systems containing Cr, V, and/or Mo. For descriptions of possibilities see chapter 3. Third part: XXIII – XXX

<table>
<tr><td>Equation: XXIII</td><td>Possibilities: 1g, 2b, 3b, 4a</td><td>Steel: Cr-V-Mo</td></tr>
<tr><td colspan="3">$$-RT\ln\frac{(1-X_{\mathrm{P}}^{\mathrm{B}})\,X_{\mathrm{P}}^{\mathrm{S}}}{X_{\mathrm{P}}^{\mathrm{B}}(1-X_{\mathrm{P}}^{\mathrm{S}})}=\Delta H_{\mathrm{P}}^{0}-\Delta S_{\mathrm{P}}^{0}T+\alpha'_{\mathrm{PV}}(X_{\mathrm{V}}^{\mathrm{S}}-X_{\mathrm{V}}^{\mathrm{B}})+\alpha'_{\mathrm{PMo}}(X_{\mathrm{Mo}}^{\mathrm{S}}-X_{\mathrm{Mo}}^{\mathrm{B}})$$</td></tr>
<tr><td>Equation: XXIV</td><td>Possibilities: 1g, 2b, 3a, 4a</td><td>Steel: Cr-V-Mo</td></tr>
<tr><td colspan="3">$$\begin{gathered}-RT\ln\frac{(1-X_{\mathrm{P}}^{\mathrm{B}})\,X_{\mathrm{P}}^{\mathrm{S}}}{X_{\mathrm{P}}^{\mathrm{B}}(1-X_{\mathrm{P}}^{\mathrm{S}})}=\\=\Delta H_{\mathrm{P}}^{0}-\Delta S_{\mathrm{P}}^{0}T-2\alpha_{\mathrm{PFe}}(X_{\mathrm{P}}^{\mathrm{S}}-X_{\mathrm{P}}^{\mathrm{B}})+\alpha'_{\mathrm{PV}}(X_{\mathrm{V}}^{\mathrm{S}}-X_{\mathrm{V}}^{\mathrm{B}})+\alpha'_{\mathrm{PMo}}(X_{\mathrm{Mo}}^{\mathrm{S}}-X_{\mathrm{Mo}}^{\mathrm{B}})\end{gathered}$$</td></tr>
<tr><td>Equation: XXV</td><td>Possibilities: 1g, 2a, 3b, 4a</td><td>Steel: Cr-V-Mo</td></tr>
<tr><td colspan="3">$$\begin{gathered}-RT\ln\frac{(1-X_{\mathrm{P}}^{\mathrm{B}}-X_{\mathrm{V}}^{\mathrm{B}}-X_{\mathrm{Mo}}^{\mathrm{B}})\,X_{\mathrm{P}}^{\mathrm{S}}}{X_{\mathrm{P}}^{\mathrm{B}}(1-X_{\mathrm{P}}^{\mathrm{S}}-X_{\mathrm{V}}^{\mathrm{S}}-X_{\mathrm{Mo}}^{\mathrm{S}})}=\\=\Delta H_{\mathrm{P}}^{0}-\Delta S_{\mathrm{P}}^{0}T+\alpha'_{\mathrm{PV}}(X_{\mathrm{V}}^{\mathrm{S}}-X_{\mathrm{V}}^{\mathrm{B}})+\alpha'_{\mathrm{PMo}}(X_{\mathrm{Mo}}^{\mathrm{S}}-X_{\mathrm{Mo}}^{\mathrm{B}})\end{gathered}$$</td></tr>
<tr><td>Equation: XXVI</td><td>Possibilities: 1g, 2a, 3a, 4a</td><td>Steel: Cr-V-Mo</td></tr>
<tr><td colspan="3">$$\begin{gathered}-RT\ln\frac{(1-X_{\mathrm{P}}^{\mathrm{B}}-X_{\mathrm{V}}^{\mathrm{B}}-X_{\mathrm{Mo}}^{\mathrm{B}})\,X_{\mathrm{P}}^{\mathrm{S}}}{X_{\mathrm{P}}^{\mathrm{B}}(1-X_{\mathrm{P}}^{\mathrm{S}}-X_{\mathrm{V}}^{\mathrm{S}}-X_{\mathrm{Mo}}^{\mathrm{S}})}=\\=\Delta H_{\mathrm{P}}^{0}-\Delta S_{\mathrm{P}}^{0}T-2\alpha_{\mathrm{PFe}}(X_{\mathrm{P}}^{\mathrm{S}}-X_{\mathrm{P}}^{\mathrm{B}})+\alpha'_{\mathrm{PV}}(X_{\mathrm{V}}^{\mathrm{S}}-X_{\mathrm{V}}^{\mathrm{B}})+\alpha'_{\mathrm{Mo}}(X_{\mathrm{Mo}}^{\mathrm{S}}-X_{\mathrm{Mo}}^{\mathrm{B}})\end{gathered}$$</td></tr>
<tr><td>Equation: XXVII</td><td>Possibilities: 1h, 2b, 3b, 4a</td><td>Steel: Cr-V-Mo</td></tr>
<tr><td colspan="3">$$\begin{gathered}-RT\ln\frac{(1-X_{\mathrm{P}}^{\mathrm{B}})\,X_{\mathrm{P}}^{\mathrm{S}}}{X_{\mathrm{P}}^{\mathrm{B}}(1-X_{\mathrm{P}}^{\mathrm{S}})}=\\=\Delta H_{\mathrm{P}}^{0}-\Delta S_{\mathrm{P}}^{0}T+\alpha'_{\mathrm{PCr}}(X_{\mathrm{Cr}}^{\mathrm{S}}-X_{\mathrm{Cr}}^{\mathrm{B}})+\alpha'_{\mathrm{PV}}(X_{\mathrm{V}}^{\mathrm{S}}-X_{\mathrm{V}}^{\mathrm{B}})+\alpha'_{\mathrm{PV}}(X_{\mathrm{Mo}}^{\mathrm{S}}-X_{\mathrm{Mo}}^{\mathrm{B}})\end{gathered}$$</td></tr>
<tr><td>Equation: XXVIII</td><td>Possibilities: 1h, 2b, 3a, 4a</td><td>Steel: Cr-V-Mo</td></tr>
<tr><td colspan="3">$$\begin{gathered}-RT\ln\frac{(1-X_{\mathrm{P}}^{\mathrm{B}})\,X_{\mathrm{P}}^{\mathrm{S}}}{X_{\mathrm{P}}^{\mathrm{B}}(1-X_{\mathrm{P}}^{\mathrm{S}})}=\Delta H_{\mathrm{P}}^{0}-\Delta S_{\mathrm{P}}^{0}T-\\-2\alpha_{\mathrm{PFe}}(X_{\mathrm{P}}^{\mathrm{S}}-X_{\mathrm{P}}^{\mathrm{B}})+\alpha'_{\mathrm{PCr}}(X_{\mathrm{Cr}}^{\mathrm{S}}-X_{\mathrm{Cr}}^{\mathrm{B}})+\alpha'_{\mathrm{PV}}(X_{\mathrm{V}}^{\mathrm{S}}-X_{\mathrm{V}}^{\mathrm{B}})+\alpha'_{\mathrm{PMo}}(X_{\mathrm{Mo}}^{\mathrm{S}}-X_{\mathrm{Mo}}^{\mathrm{B}})\end{gathered}$$</td></tr>
<tr><td>Equation: XXIX</td><td>Possibilities: 1h, 2a, 3b, 4a</td><td>Steel: Cr-V-Mo</td></tr>
<tr><td colspan="3">$$\begin{gathered}-RT\ln\frac{(1-X_{\mathrm{P}}^{\mathrm{B}}-X_{\mathrm{Cr}}^{\mathrm{B}}-X_{\mathrm{V}}^{\mathrm{B}}-X_{\mathrm{Mo}}^{\mathrm{B}})\,X_{\mathrm{P}}^{\mathrm{S}}}{X_{\mathrm{P}}^{\mathrm{B}}(1-X_{\mathrm{P}}^{\mathrm{S}}-X_{\mathrm{Cr}}^{\mathrm{S}}-X_{\mathrm{V}}^{\mathrm{B}}-X_{\mathrm{Mo}}^{\mathrm{S}})}=\\=\Delta H_{\mathrm{P}}^{0}-\Delta S_{\mathrm{P}}^{0}T+\alpha'_{\mathrm{PCr}}(X_{\mathrm{Cr}}^{\mathrm{S}}-X_{\mathrm{Cr}}^{\mathrm{B}})+\alpha'_{\mathrm{PV}}(X_{\mathrm{V}}^{\mathrm{S}}-X_{\mathrm{V}}^{\mathrm{B}})+\alpha'_{\mathrm{PMo}}(X_{\mathrm{Mo}}^{\mathrm{S}}-X_{\mathrm{Mo}}^{\mathrm{B}})\end{gathered}$$</td></tr>
<tr><td>Equation: XXX</td><td>Possibilities: 1h, 2a, 3a, 4a</td><td>Steel: Cr-V-Mo</td></tr>
<tr><td colspan="3">$$\begin{gathered}-RT\ln\frac{(1-X_{\mathrm{P}}^{\mathrm{B}}-X_{\mathrm{Cr}}^{\mathrm{B}}-X_{\mathrm{V}}^{\mathrm{B}}-X_{\mathrm{Mo}}^{\mathrm{B}})\,X_{\mathrm{P}}^{\mathrm{S}}}{X_{\mathrm{P}}^{\mathrm{B}}(1-X_{\mathrm{P}}^{\mathrm{S}}-X_{\mathrm{Cr}}^{\mathrm{S}}-X_{\mathrm{V}}^{\mathrm{B}}-X_{\mathrm{Mo}}^{\mathrm{S}})}=\Delta H_{\mathrm{P}}^{0}-\Delta S_{\mathrm{P}}^{0}T-\\-2\alpha_{\mathrm{PFe}}(X_{\mathrm{P}}^{\mathrm{S}}-X_{\mathrm{P}}^{\mathrm{B}})+\alpha'_{\mathrm{PCr}}(X_{\mathrm{Cr}}^{\mathrm{S}}-X_{\mathrm{Cr}}^{\mathrm{B}})+\alpha'_{\mathrm{V}}(X_{\mathrm{V}}^{\mathrm{S}}-X_{\mathrm{V}}^{\mathrm{B}})+\alpha'_{\mathrm{Mo}}(X_{\mathrm{Mo}}^{\mathrm{S}}-X_{\mathrm{Mo}}^{\mathrm{B}})\end{gathered}$$</td></tr>
</table>

multicomponent system. Gibbs free energy for dilute binary m-i system, ΔG_i^0, is expressed by means of corresponding enthalpy (ΔH_i^0) and entropy (ΔS_i^0) terms (compare Eqs. 3 and 5). Measure of interactions is characterised by α_{im} (binary) and α'_{ij} (ternary) coefficients.

With respect to the elements detected at grain boundaries (see chapter 2 of the present paper), altogether six thermodynamic parameters characterising equilibrium segregation of phosphorus in the investigated steels can be determined: $\Delta H_{\mathrm{P}}^{0}$, $\Delta S_{\mathrm{P}}^{0}$, α_{PFe}, α'_{PCr}, α'_{PMo}, and α'_{PV}. To calculate them, the Langmuir-McLean equation (2) and various modifications of the Guttmann equations (4) and (5) can be used. In creation of the equations four principal criteria were taken into account:

1. *Number of components in a system.* The investigated steels were piecemeal considered to be Fe-P (**1a**), Fe-P-Cr (**1b**), Fe-P-V (**1c**), Fe-P-Mo (**1d**), Fe-P-Cr--V (**1e**), Fe-P-Cr-Mo (**1f**), Fe-P-V-Mo (**1g**), or Fe-P-Cr-V-Mo (**1h**) systems. Mn, Si, S, and N were not found to segregate at grain boundaries, C was neglected because of contamination from the residual gas atmosphere and the occurrence in intergranular carbide particles.

2. *Considering* (**2a**) *or neglecting* (**2b**) *the site competition effect* between phosphorus and alloying elements (Cr, Mo, V).

3. *Considering* (**3a**) *or neglecting* (**3b**) *the Fowler type binary interaction* (P-P).

4. *Considering* (**4a**) *or neglecting* (**4b**) *the ternary type interactions* (P-Cr, P-Mo, P-V).

Symbols **1a-1h**, **2a-2b**,**3a-3b**, and **4a-4b** were used to distinguish between individual possibilities in the frame of each criterion. If combine the possibilities, altogether 30 equations can be created, see Tables 2–4. To distinguish between them, each equation is labelled by a Roman number and characterised by a set of symbols reflecting the possibilities chosen. Applicability of the equations for the investigated Cr, Cr-V, and Cr-V-Mo steels is also marked in Tables 2–4.

4. Results of thermodynamic calculations

Five thermodynamic parameters: $\Delta H_{\mathrm{P}}^{0}$, $\Delta S_{\mathrm{P}}^{0}$, α'_{PCr}, α'_{PMo}, and α'_{PV}, were calculated according to the odd numbered Eqs. I, III, V, VII, IX, XI, XIII, XV, XVII, XIX, XXI, XXIII, XXV, XXVII, and XXIX (Tables 2–4) using the method of multiple linear regression. Originally exponential equations (all derived from Eq. 4) were transformed by logarithmic treatment to the linear form. Experimentally determined values of the grain boundary and bulk concentrations of P, Cr, Mo, V, and Fe as well as ageing temperatures were used as input data. For each condition at least 8 Auger spectra from intergranular facets were collected. The occurrence of carbide particles at grain boundaries was not considered in Cr, V, and Mo peak heights. To specify the final grain boundary concentration, the even partitioning of segregating species between both adjacent grains (factor 2) was considered. Fitting the experimental data by Eqs. I, III, V, VII, IX, XI, XIII, XV, XVII, XIX, XXI, XXIII, XXV, XXVII, and XXIX showed good correlation. The corresponding correlation coefficients ranged between 0.85 and 0.98.

Table 5. Thermodynamic parameters of phosphorus segregation for Cr steel. There are compared results calculated according to different equations

Equation	$\Delta H_{\mathrm{P}}^{0}$ [kJ·mol^{-1}]	$\Delta S_{\mathrm{P}}^{0}$ [J·mol^{-1}·K^{-1}]	α'_{PCr} [kJ·mol^{-1}]
I	−35	4	
III	−31	8	−15
V	−31	8	−24

Table 6. Thermodynamic parameters of phosphorus segregation for Cr-V steel. There are compared results calculated according to different equations

Equation	$\Delta H_{\mathrm{P}}^{0}$ [kJ·mol^{-1}]	$\Delta S_{\mathrm{P}}^{0}$ [J·mol^{-1}·K^{-1}]	α'_{PCr} [kJ·mol^{-1}]	α'_{PV} [kJ·mol^{-1}]
I	−32	9		
III	−32	9	−19	
V	−32	9	−10	
VII	−33	7		−34
IX	−33	7		−44
XV	−33	5	−37	−39
XVII	−34	4	−47	−50

Table 7. Thermodynamic parameters of phosphorus segregation for Cr-V-Mo steel. There are compared results calculated according to different equations

Equation	$\Delta H_{\mathrm{P}}^{0}$ [kJ·mol^{-1}]	$\Delta S_{\mathrm{P}}^{0}$ [J·mol^{-1}·K^{-1}]	α'_{PCr} [kJ·mol^{-1}]	α'_{PV} [kJ·mol^{-1}]	α'_{PMo} [kJ·mol^{-1}]
I	−23	17			
III	−21	16	−64		
V	−21	16	−73		
VII	−29	8		−50	
IX	−29	8		−58	
XI	−13	25			−81
XIII	−12	26			−90
XV	−25	11	−56	−27	
XVII	−25	11	−66	−36	
XIX	−14	22	−50		−62
XXI	−13	23	−60		−73
XXIII	−16	21		−18	−71
XXV	−16	21		−28	−81
XXVII	−14	22	−50	−2	−61
XXIX	−13	22	−60	−12	−72

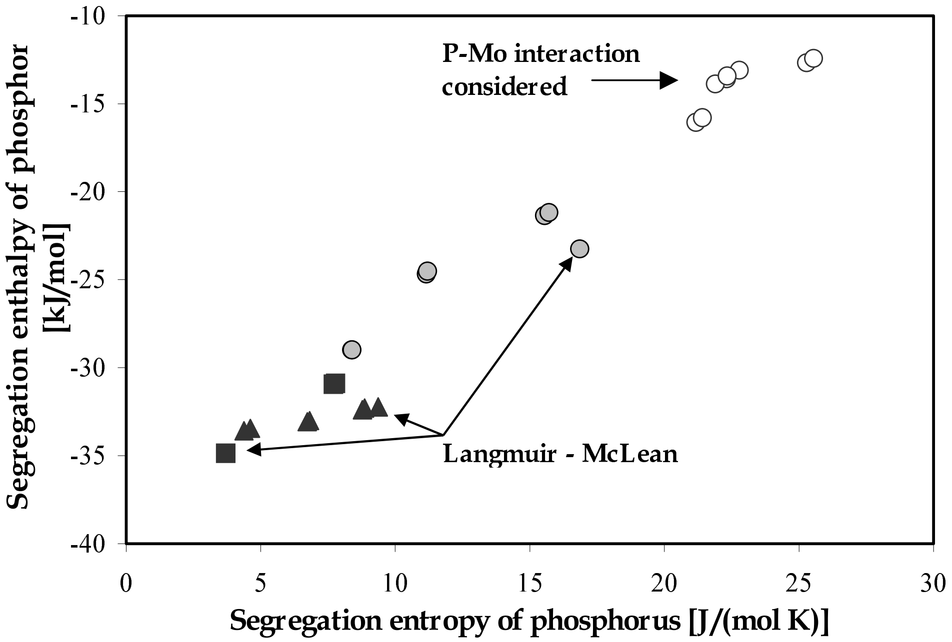

Fig. 2. Enthalpy of phosphorus segregation plotted as a function of entropy. Couples of parameters calculated according to Eqs. I, III, V, VII, IX, XI, XIII, XV, XVII, XIX, XXI, XXIII, XXV, XXVII, or XXIX (Tables 2–4) are illustrated by following symbols: ■ (Cr steel), ▲ (Cr-V steel), and ◎, ○ (Cr-V-Mo steel). The P-Mo interaction was only considered in calculations attributed to empty circles.

The last of thermodynamic parameters, α_{PFe} (see chapter 3), was not determined, because the consideration of Fowler term led to the physically meaningless results as reported earlier in works [23–25]. Therefore, the even numbered equations in Tables 2–4 were not used for calculations in the present work.

The values of ΔH^0_{P}, ΔS^0_{P}, α'_{PCr} determined for Cr, Cr-V, and Cr-V-Mo steels are given in respective Tables 5, 6, and 7. As compared to Table 5, the values of α'_{PV} are moreover included in Table 6. Table 7, pertinent to the Cr-V-Mo steel, contains the values of all thermodynamic parameters fitted. A relationship between the enthalpy and entropy of phosphorus segregation for all the investigated steels is illustrated in Fig. 2. In Fig. 3, energy terms (ΔH^0_{P}, α'_{PCr}, α'_{PMo}, and α'_{PV}) are plotted as functions of phosphorus segregation entropy. Points corresponding to the different steels are marked by different symbols.

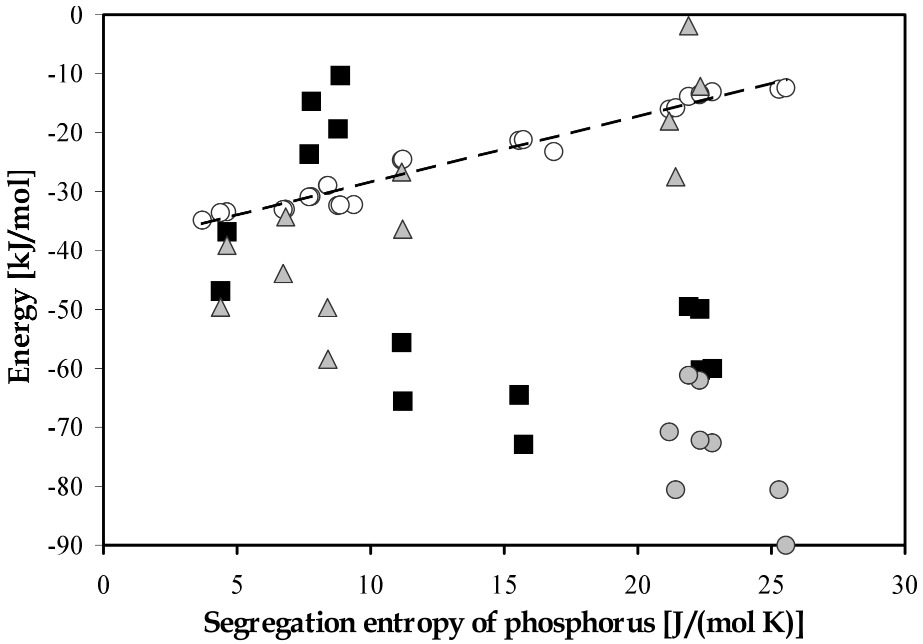

Fig. 3. Energy terms: enthalpy of phosphorus segregation (○), P-Cr interaction coefficient (■), P-V interaction coefficient (△), and P-Mo interaction coefficient (●), plotted as a function of entropy. Symbols represent couples of parameters calculated according to Eqs. I, III, V, VII, IX, XI, XIII, XV, XVII, XIX, XXI, XXIII, XXV, XXVII, or XXIX for all investigated steels (Tables 2–4). Dashed line in upper part of the plot illustrates linear relationship between enthalpy and entropy of phosphorus segregation.

5. Discussion

Before concluding the results of the investigation, it should be reasonable to summarise shortly the marginal conditions of experiments and calculations:

1. Experimental measurements were done at two temperatures (773 and 823 K). For the precise determination of thermodynamic parameters a number of temperatures is rather small, but mathematically sufficient.

2. To characterise the influence of alloying elements (Cr, V, and Mo) on phosphorus grain boundary segregation, three types of low alloy steels (alloyed with only Cr, Cr + V, and Cr + V + Mo) with comparable bulk phosphorus contents (0.040–0.045 % in mass) were experimentally investigated.

3. Ageing for 5000 h at temperatures above 823 K was sufficient to reach the equilibrium values of grain boundary concentration applicable in thermodynamic calculations.

4. The neglect of carbon originated from intergranular carbide particles does not influence the calculated thermodynamic parameters significantly [1, 26].

5. The values of ternary interaction coefficients can be partially influenced by the use of the non-corrected Cr, V, and Mo Auger peak heights, because the occurrence of the mentioned metallic elements in intergranular particles is well-known [1].

The results achieved were evaluated from three points of view: changes in phosphorus segregation enthalpy, relationship between enthalpy and entropy of phosphorus segregation, and changes in ternary interaction coefficients.

5.1 Changes in segregation enthalpy of phosphorus

The values of $\Delta H_{\mathrm{P}}^{0}$ calculated for the Cr and Cr-V steels according to the different equations range between -35 and -31 kJ·mol^{-1} (Tables 5 and 6) what is in good agreement with the results published earlier for similar materials [24, 27, 28]. Between the values calculated according to Eq. I (Langmuir-McLean) and other equations, small differences were only found, Fig. 2. This indicates the consideration of P-Cr (P-V) interactions for the Cr and Cr-V steels does not play any important role in influencing the $\Delta H_{\mathrm{P}}^{0}$ values.

A bit different situation was recorded for the Cr-V-Mo steel. The presence of molybdenum in the steel probably contributes to the decrease in the phosphorus grain boundary concentration [20], and makes in this way $\Delta H_{\mathrm{P}}^{0}$ values less negative. According to Eq. I (Langmuir-McLean), $\Delta H_{\mathrm{P}}^{0} = -22$ kJ·mol^{-1} (Table 7, Fig. 2). Similar values were determined earlier by Hänzel and Grabke for Fe-P alloys [29] and Janovec et al. for Cr-Mo-V steel [23]. A scatter of $\Delta H_{\mathrm{P}}^{0}$ values for the Cr-V--Mo steel is evidently higher than for other two investigated steels. The mentioned values fluctuate between -29 and -12 kJ·mol^{-1} where the value corresponding to the Langmuir-McLean equation lies approximately in the middle of this range. If P-Cr and/or P-V ternary interactions were considered in the calculations, the $\Delta H_{\mathrm{P}}^{0}$ values ranged between -29 and -21 kJ·mol^{-1} (gray circles in Fig. 2). A consideration of the P-Mo interaction has shifted $\Delta H_{\mathrm{P}}^{0}$ values to the less negative region (empty circles in Fig. 2). This is the indirect evidence of the influence of molybdenum on the values of phosphorus segregation enthalpy.

With respect to the literature data [23, 24, 27–29], the values of $\Delta H_{\mathrm{P}}^{0}$ calculated for the Cr and Cr-V steels as well as for the Cr-V-Mo steel according to Eqs. I, VII, IX, XV, or XVII are representative. In all the mentioned cases, no P-Mo interactions were considered. The corresponding $\Delta S_{\mathrm{P}}^{0}$ values were found to be rather smaller (they range between 3 and 17 J·mol^{-1}·K^{-1}).

5.2 Relationship between enthalpy and entropy of phosphorus segregation

As is evident from Fig. 2, there exists the tendency to a linear relationship between the calculated values of segregation enthalpy and entropy. This phenomenon was described earlier by Rittner and Seidman [30] for segregation of paladium in nickel and Lejček et al. [31–33] for segregation of phosphorus, carbon, and silicon in iron-base alloys. In both cases, segregation enthalpies and entropies for differently oriented grain boundaries were calculated. The phenomenon was attributed to the existence of compensation temperature at which Gibbs energy of segregation is the same for all grain boundaries [34]. In the present work enthalpies and entropies of phosphorus segregation were calculated for three different steels with unidentified, mostly general grain boundaries according to 15 different equations. Variations in both the steel chemical composition and the form of segregation equations revealed considerable changes in the values of $\Delta H_{\mathrm{P}}^{0}$ and $\Delta S_{\mathrm{P}}^{0}$, but the linear relationship between them was kept. However, it should be distinguished between the linear relationship achieved by means of different ways of data correlation in the present work and that mentioned in works [30–33]. In the latter case, points constituting the linear relationship represent mutual dependence of experimental values of $\Delta H_{\mathrm{I}}^{0}$ and $\Delta S_{\mathrm{I}}^{0}$ for different grain boundary positions [30] and for differently oriented grain boundaries [31–33]. The relationship has therefore the strictly defined physical meaning.

For each of the investigated steels, individual values of $\Delta H_{\mathrm{I}}^{0}$ and $\Delta S_{\mathrm{I}}^{0}$ were achieved from the same temperature dependence of phosphorus grain boundary concentration using different ways of the correlation. Thus, no all of the calculated values can be interpreted as true values of standard molar thermodynamic parameters [16]. With respect to the objectives of the present work, it is impossible to determine which of the $\Delta H_{\mathrm{I}}^{0}$ and $\Delta S_{\mathrm{I}}^{0}$ values possess the physical meaning of the standard molar thermodynamic parameter of grain boundary segregation.

5.3 Changes in ternary interaction coefficients

The fitted values of ternary interaction coefficients differ from each other substantially, Fig. 3. For instance, the values of α'_{PCr} calculated for the Cr-V steel according to different equations range between -47 and -10 kJ$\cdot$mol^{-1}, Table 6. The corresponding values of $\Delta H_{\mathrm{P}}^{0}$ are about -33 kJ$\cdot$mol^{-1}. With respect to their higher scatter it is impossible to find some unambiguous physical interpretation for fitted values of the interaction coefficient. If the most positive value of α'_{PCr} is taken in account, very weak (practically negligible) P-Cr interaction can be predicted what is in agreement with earlier observations of Janovec et al. [23, 24]. The acceptance of the most negative α'_{PCr} value implicates a strong P-Cr co-segregation as reported by Guttmann [28]. The extension of the analysis to all values of α'_{PCr} (calculated also for Cr and Cr-V-Mo steels) confirmed the impossibility to give unambiguous physical statement to the P-Cr interaction in the investigated steels because of an enormous scatter of the fitted parameters.

For α'_{PV} and α'_{PMo} coefficients a comparable high scatter of calculated values was recorded as presented above for the α'_{PCr} coefficient. Between the values of α'_{PV} and ΔH^0_{P} a positive correlation was found (see corresponding dependence in Fig. 3) what indicates a proportional participation of the attractive P-V interaction in promotion of phosphorus segregation. This is physically acceptable, because the shift of phosphorus segregation enthalpy to less negative values is accompanied by the weakening of the P-V attractive interaction (corresponding α'_{PV} values become also less negative). On the other hand, the negative correlation was found between α'_{PCr} (α'_{PMo}) values and ΔH^0_{P} in dependence on segregation entropy. Physical interpretation of this fact is controversial, because an extrapolation of ΔH^0_{P} to positive values should deepen the negativity of extrapolated α'_{PCr} and α'_{PMo} coefficients. Thus, the phosphorus desegregation ($\Delta H^0_{\mathrm{P}} > 0$) should be strengthened by strong P-Cr and/or P-Mo attractive interactions (α'_{PCr}, $\alpha'_{\mathrm{PMo}} \ll 0$). The last suggestion seems to be physically unacceptable, because at least Mo is known as a promoter of phosphorus segregation (there was proposed theory of so-called P-Mo co-segregation) in alloy steels [28].

A high scatter of the values of interaction coefficients calculated for the investigated steels according to the different segregation equations gives rise a shadow of doubt, if the Guttmann type equations reflecting the ternary interactions are suitable for the calculations of interaction coefficients for alloy steels. It was shown in the present work that the higher a number of ternary interactions considered the higher a scatter of values of interaction coefficient (Fig. 3). The presence of carbide particles at analysed grain boundaries (they could contribute to the Cr, V, Mo peak heights in Auger spectra), no consideration of possible phosphide formation [28, 35], and a lack of information about crystallography of analysed mostly random boundaries prevent from the generalisation of the above findings.

6. Conclusions

To specify the ability of different segregation equations for the quantification of phosphorus segregation three low alloy steels (alloyed with only Cr, Cr + V, and Cr + V + Mo) with comparable bulk phosphorus contents (0.040–0.045 % in mass) were investigated after ageing at 773 and 823 K. The results of experimental measurements and thermodynamic calculations can be summarised as follows:

1. It was shown that the consideration of P-Cr and P-V interactions does not play any important role in influencing the ΔH^0_{P} values for the Cr and Cr-V steels. If considered the P-Mo interaction in the Cr-V-Mo steel, the values of ΔH^0_{P} became less negative.

2. Variations in both the steel chemical composition and the form of segregation equations revealed considerable changes in values of ΔH^0_{P} and ΔS^0_{P}, but the linear relationship between them was kept.

3. There was recorded a high scatter of α'_{PCr}, α'_{PV}, and α'_{PMo} values calculated according to the different segregation equations. It was shown that the higher a number of ternary interactions considered the higher a scatter of the values of interaction coefficients.

Acknowledgements

The present work was supported by the Grant Agency of the Slovak Republic (VEGA) under grant No. 2/1062/21. Authors of the work express thanks to Dr. Pavel Lejček for valuable comments and useful advice.

REFERENCES

[1] JANOVEC, J.: Nature of alloy steel intergranular embrittlement. Bratislava, VEDA 1999.

[2] READ, W. T.—SHOCKLEY, W.: Phys. Rev., *78*, 1950, p. 275.

[3] READ, W. T.: Dislocations in crystals. New York, McGraw-Hill 1953.

[4] SMITH, D. A.—POND, R. C.: Inter. Met. Rev., *205*, 1976, p. 61.

[5] SHEWMON, P.: Diffusion in solids. Warrendale, TMS 1989.

[6] BUERGER, M. J.: Contemporary crystallography. New York, Mc Graw-Hill 1970.

[7] ROSENHAIN, W.—EWEN, D.: J. Inst. Metals, *8*, 1912, p. 149.

[8] HARGREAVES, F.—HILLS, R. J.: J. Inst. Metals, *41*, 1929, p. 257.

[9] KRONBERG, M. L.—WILSON, F. H.: Trans. AIME, *185*, 1949, p. 501.

[10] POTAPOV, L. P.—GLOWIN, B. F.—SHIRYAEV, P. H.: Fiz. Met. Metalloved., *32*, 1971, p. 227.

[11] POND, R. C.—VITEK, V.: Proc. Roy. Soc., *A357*, 1977, p. 453.

[12] HERRING, C.: Structure and properties of solid surfaces. Chicago, University of Chicago Press 1953.

[13] YIP, S.—WOLF, D.: Mater. Sci. Forum, *46*, 1989, p. 77.

[14] GIBBS, J. W.: Scientific Papers, *i (Thermodynamics)*, 1906, p. 219.

[15] GUGGENHEIM, E. A.: Thermodynamics (2$^{\mathrm{nd}}$ edition). Amsterdam, North-Holland 1950.

[16] McLEAN, D.: Grain boundaries in metals. London, Oxford University Press 1957.

[17] GUTTMANN, M.: Surface Sci., *53*, 1975, p. 213.

[18] GUTTMANN, M.—McLEAN, D.: Interfacial segregation. Ohio, ASM 1979, p. 216.

[19] SEAH, M. P.: Acta Metall., *25*, 1977, p. 345.

[20] McMAHON, C. J. Jr.: Mater. Sci. Forum, *48*, 1989, p. 61.

[21] PERHÁČOVÁ, J.—GRMAN, D.—SVOBODA, M.—PATSCHEIDER, J.—VÝROSTKOVÁ, A.—JANOVEC, J.: Mater. Letters, *47*, 2001, p. 44.

[22] DAVIS, L. E.—McDONALD, M. C.—PALMBERG, P. W.—RIACH, G. R.—WEBER, R. A.: Handbook of Auger electron spectroscopy (2$^{\mathrm{nd}}$ edition). Minnesota, Phys. Electronic Industries 1976.

[23] JANOVEC, J.—GRMAN, D.—MAGULA, V.—PATSCHEIDER, J.—LEJČEK, P.—ŠEVC, P.—BLACH, J.: J. Surf. Sci., *5*, 1999, p. 294.

[24] JANOVEC, J.: Kovove Mater., *37*, 1999, p. 165.

[25] JANOVEC, J.—GRMAN, D.—PERHÁČOVÁ, J.—LEJČEK, P.—PATSCHEIDER, J.—ŠEVC, P.: Surf. Interface Anal., *30*, 2000, p. 354.

[26] JANOVEC, J.—VÝROSTKOVÁ, A.—PERHÁČOVÁ, J.—HOMOLOVÁ, V.—GRABKE, H. J.—ŠEVC, P.—LUCAS, M.: Steel Res., *70*, 1999, p. 269.

[27] ERHART, H.—GRABKE, H. J.: Met. Sci., *15*, 1981, p. 401.
[28] GUTTMANN, M.—DUMOULIN, Ph.—WAYMAN, M.: Metall. Trans., *13A*, 1982, p. 1693.
[29] HÄNSEL, H—GRABKE, H. J.: Scripta Metall., *20*, 1986, p. 1641.
[30] RITTNER, J.—SEIDMAN, D.: Acta Mater., *45*, 1997, p. 3191.
[31] LEJČEK, P.: Surf. Interface. Anal., *26*, 1998, p. 800.
[32] LEJČEK, P.: J. Phys. France IV, 9, 1999, p. 21.
[33] P. ŠEVC—JANOVEC, J.—LEJČEK, P.—ZÁHUMENSKÝ, P.—BLACH, J.: Scripta Mater., *46*, 2002, p. 7.
[34] GOTTSTEIN, G.—MOLODOV, D. A.—SHVINDLERMAN, L. S.: Interface Sci., *6*, 1998, p. 7.
[35] ŠEVC, P.—MANDRINO, D.—BLACH, J.—JENKO, M.—JANOVEC, J.: Kovove Mater., *40*, 2002, p. 35.

Received: 17.4.2002